Available online at www.sciencedirect.com
ScienceDirect
Composite Structures 76 (2006) 52–61
COMPOSITE STRUCTURES
www.elsevier.com/locate/compstruct

Structural testing and numerical simulation of a 34 m composite wind turbine blade

F.M. Jensen [a,*], B.G. Falzon [b], J. Ankersen [b], H. Stang [c]

[a] Department of Wind Energy, Risoe National Laboratory, P.O. Box 49, Roskilde, Denmark
[b] Department of Aeronautics, Imperial College London, South Kensington Campus, London SW7 2AZ, UK
[c] Department of Civil Engineering, Technical University of Denmark, Lyngby, Denmark

Available online 12 July 2006

Abstract

A full-scale 34 m composite wind turbine blade was tested to failure under flap-wise loading. Local displacement measurement equipment was developed and displacements were recorded throughout the loading history.

Ovalization of the load carrying box girder was measured in the full-scale test and simulated in non-linear FE-calculations. The non-linear Brazier effect is characterized by a crushing pressure which causes the ovalization. To capture this effect, non-linear FE-analyses at different scales were employed. A global non-linear FE-model of the entire blade was prepared and the boundaries to a more detailed sub-model were extracted. The FE-model was calibrated based on full-scale test measurements.

Local displacement measurements helped identify the location of failure initiation which lead to catastrophic failure. Comparisons between measurements and FE-simulations showed that delamination of the outer skin was the initial failure mechanism followed by delamination buckling which then led to collapse.

Keywords: Structural testing; Wind turbine blades; Non-linear finite element analysis; Sub-modelling; Failure mechanism; Brazier effect; Anticlastic effect

1. Introduction

The size of wind turbine blades are expected to increase considerably in the future, demanding a better understanding of the structural behaviour on a different scale. Detailed structural behaviour must be investigated beyond the elastic range. This may include the identification of failure modes which lead to ultimate collapse. Wind turbine blades have typically been optimized by experimental tests and simplified analytical methods. However, numerical simulation tools are gaining wider acceptance as they become more sophisticated in their predictive capability as well as offering a route to significantly lower developmental costs.

2. Numerical methods

The finite element method (FEM) has traditionally been used in the development of wind turbine blades mainly to investigate the global behaviour in terms of, for example, eigenfrequencies, tip deflections, and global stress/strain levels. This type of FE-simulation usually predicts the global stiffness and stresses with a good accuracy. Local deformations and stresses are often more difficult to predict and little has been published in this area. One reason is that the highly localised deformations and stresses can be non-linear, while the global response appears linear for relatively small deflections. Another factor is that a relatively simple shell model can be used for representing the global behaviour, while a computationally more expensive 3D-solid model may be necessary to predict this localised behaviour.

Even with a highly detailed 3D solid model it would rarely be possible to predict deformations or stresses accurately without calibration of the FE-model. This

* Corresponding author.
E-mail address: find.moelholt.jensen@risoe.dk (F.M. Jensen).

0263-8223/$ - see front matter © 2006 Elsevier Ltd. All rights reserved.
doi:10.1016/j.compstruct.2006.06.008

calibration is necessary due to large manufacturing tolerances. Features such as box girder corners and adhesive joints often differ from specifications. Geometric imperfections are often seen and can cause unexpected behaviour, especially relating to the strength predictions but also the local deformations can be affected. In this paper, box girder corners were not modelled in detail using solids. Instead, the rotational stiffness of the corners was calibrated with deflections measured in the full-scale test.

A big advantage of using FEM is that, once the model is set up and calibrated, complex load cases representing actual wind conditions can be analyzed. Only idealised loads can be imposed in a full-scale test and in this paper the critical flap-wise load case is evaluated.

3. Full-scale test of 34 m SSP-blade

A full-scale 34 m wind turbine blade, manufactured by SSP-Technology A/S, was tested to failure under flap-wise loading as shown in Fig. 1. The blade had passed all static and dynamic (correspond to 20 years life time) tests required by the classification bodies. The SSP-blade is made of glass-epoxy pre-preg material and is designed with a load carrying box girder, see Fig. 2.

Earlier experience from another full-scale test [1] and FE-simulations [2] has shown that the cap deflect non-linearly. The conclusion from these investigations is that the load carrying box girder ovalizes when the blade bends flap-wise. New equipment has been developed to record the web deflection resulting from ovalization, see Fig. 3.

Each web sensor can independently measure in- and outward web deflection which occurs when the box girder ovalizes or is subjected to other types of deformation. In the 8 m segment near the root, effects due to change in geometry interact with conventional ovalization effects resulting in a counterintuitive non-linear response. Mechanisms which explain these deformations and the relevance of including these effects are presented.

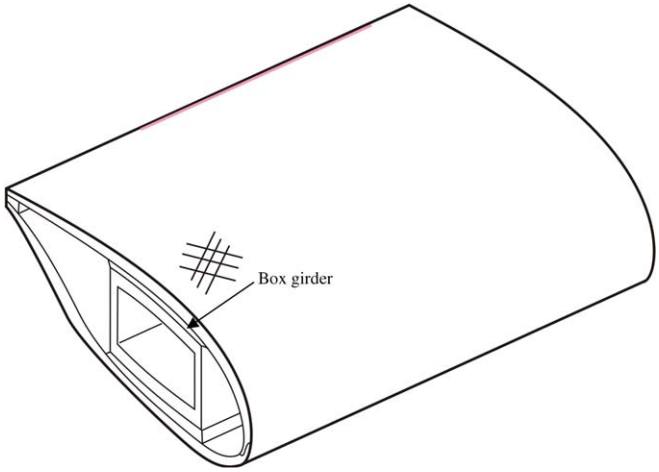

Fig. 2. Blade with a load carrying main spar.

A combination of measurements and FE-simulation has shown that delamination of the outer skin was the initial failure mechanism followed by delamination buckling which led to collapse.

4. Sub-modelling techniques

A local model, using shell and brick elements, was developed for a span-wise segment of the blade. The 0–13 m segment is found to be the most critical part and final failure also occurred in this section. The boundary conditions used in this sub-model were based on the displacement field taken from the global FE-model. Normally, the linear displacement field is used in sub-modelling techniques, but in this case this technique cannot be used, since non-linear effects dominate. The explanation as to why the use of a

Fig. 1. Full-scale test – flap-wise loading.

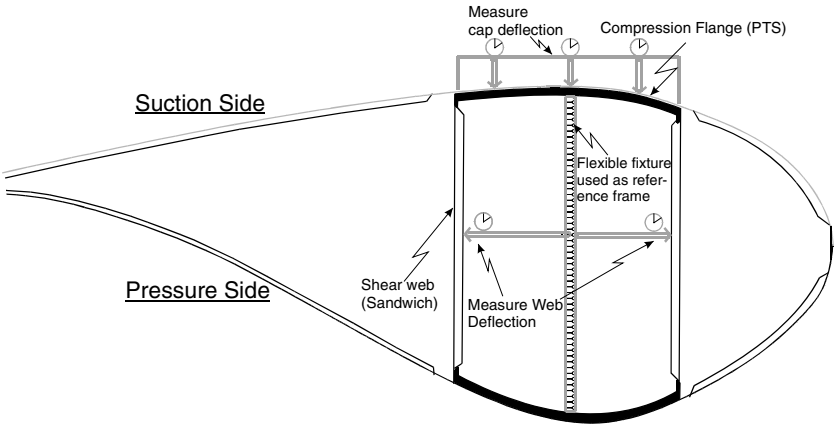

Fig. 3. Local displacement equipment in a blade section.

non-linear displacement field is required, even at moderate non-linearity, is given in this paper.

5. Experimental results

Deflections at the centre of the upper spar cap have been measured at seven different sections. In the section 10.3 m from the root, three chord-wise locations were measured, as shown in Fig. 3.

New equipment for deflection measurement was developed for use inside the box girder. The equipment is shown in Fig. 3 and measures local web deflections with a fixed reference frame in the centre of the box girder. The central reference frame is telescopic to allow for change in section height during ovalization of the box girder.

6. Non-linear geometric deformations

Different deformation patterns were observed during the full-scale test. The blade showed three distinct deformation patterns dependent on the span-wise location (all measured from the root):

- Root segment (0–4 m)
- Transition segment (4–8 m) from root to box girder segment
- Box girder segment (8–34 m)

The first two segments will only be treated very briefly in this paper, but are included to illustrate the complexity of local deformations. Deformations in the root segment also influence the boundary conditions on the box girder segment, which starts 8 m from the root. It should be noted that the box girder actually runs along the full length of the blade but behaves differently in the three segments describe in the following.

6.1. Root segment (0–4 m)

Part of the web deformations are due to the gravity load, which causes the webs to show a non-symmetric behaviour before loading. This behaviour is specific to the SSP-blade, and is due to the change in box girder section geometry along the root segment.

A sketch of the non-symmetric web deflection is shown in Fig. 4a and measurements are shown in Fig. 4b. The measurements exclude deflections due to pre-load (gravity load) because the measuring gauges were reset prior to loading of the blade. The unusual behaviour of the webs is not discussed further here but is most likely related to the constraints imposed by the stiff root connection to the hub. In the current context, it is merely of interest to be able to apply the correct boundary conditions on the segments further away from the root.

6.2. Transition segment (4–8 m)

A large change in cap curvature, and therefore cap height, takes place in the transition segment, see Fig. 5a.

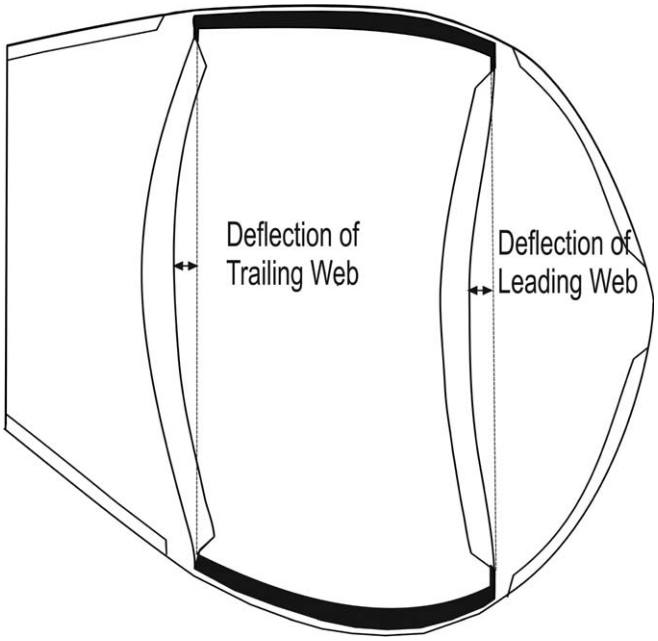

Fig. 4a. Sketch of non-symmetric.

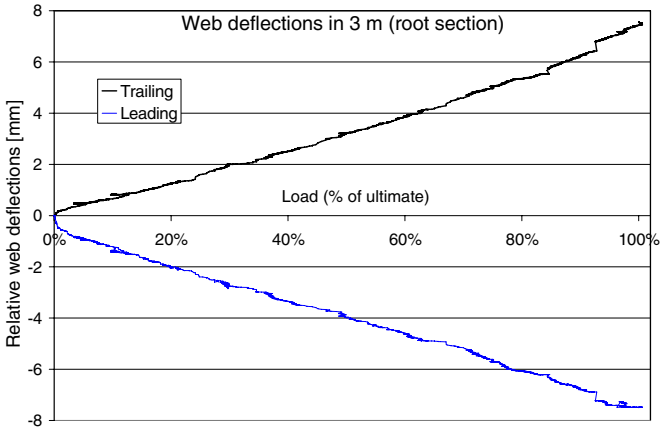

Fig. 4b. Relative web deflections versus load.

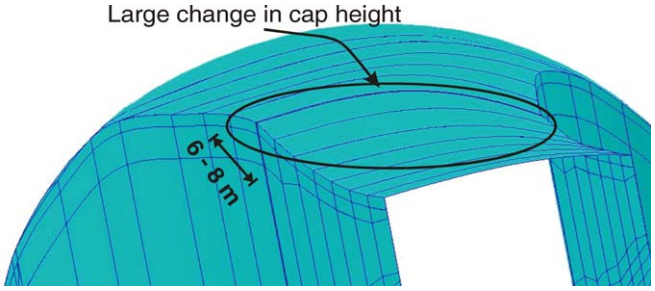

Fig. 5a. Changes in profile height.

Outward cap deformations were measured during the full-scale test as shown in Fig. 5b. These outward deflections were seen on the compression side of the blade and are linked to the rapid change in cap profile in this segment.

Box girder segment (8–34 m). In this segment the expected ovalization caused by flap-wise bending was observed. This non-linear deformation or "flattening" of the cross section is also known as the Brazier effect [1] and is most pronounced for long thin hollow beams

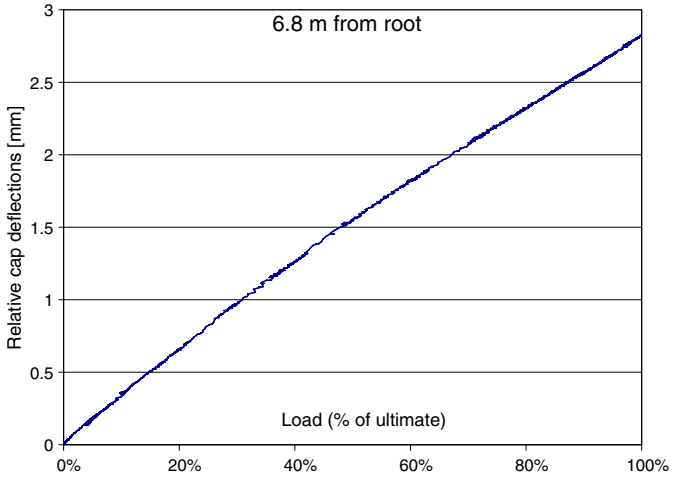

Fig. 5b. Outward cap deformation – measured.

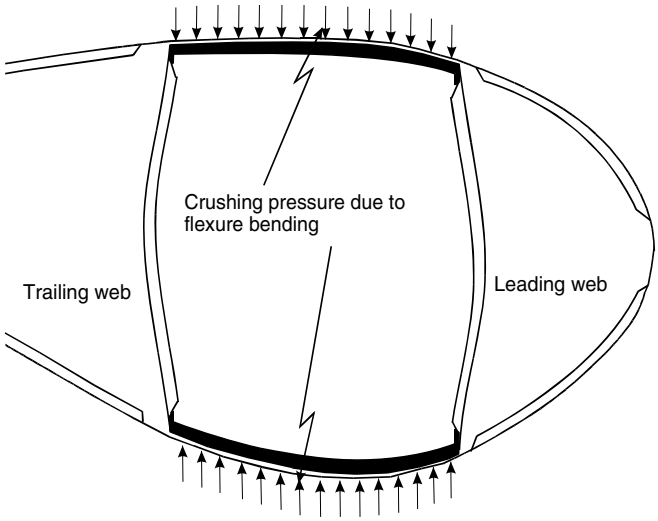

Fig. 6. Crushing pressure from the Brazier effect.

subjected to bending. The crushing pressure caused by the Brazier effect has a large effect on the web deflections and local deformation sensors have measured up to 20 mm displacement at the trailing web and 11 mm for leading web (Fig. 6).

Outer skin debonding from the box girder, see Fig. 7a, was observed after collapse, but it was not clear at which load this failure mode had occurred. A study of measured cap deflections has shown that the skin peeling starts at 92% of the ultimate load, see Fig. 7c. The jump in measured displacement is not due to sudden chord-wise bending of the cap, instead it was caused by the skin debonding from the cap where the skin assumes more of the initial curvature. The reference frame for measuring cap deflection is attached to the outer skin rather than directly to the box girder corner. Fig. 7b illustrates this observation. In Fig. 7c another skin peeling jump can be observed at 97% of ultimate load.

The actual maximum cap deformation of 4.3 mm was obtained by extrapolation, see Fig. 7c. This is the value that would have been observed if measurements were taken directly on the box girder or had debonding not occurred.

The skin debonding is expected to have a major influence on the final collapse. Buckling capacity of the blade is reduced dramatically once the outer skin and box girder separate. This buckling behaviour can be observed in Fig. 7c at 100% load, just before failure.

7. Final failure – buckling assumption

7.1. Cap and web deformations

The cap centerline deflections were measured at four span-wise positions (8.5 m, 10.3 m, 12.5 m and 15.2 m) in the box girder segment from 8 to 15 m. A 8–15 m segment of the blade is shown in Fig. 8a with the upper cap centreline indicated. The measured cap deflections are plotted in Fig. 8b. Unfortunately no measurement was taken at

Fig. 7a. Skin peeling from cap.

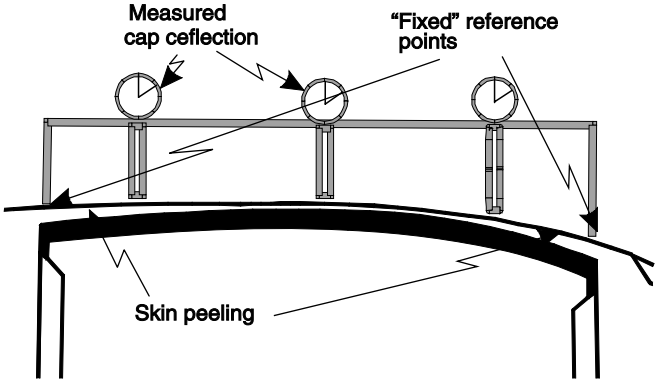

Fig. 7b. Reference points not fixed after skin peeling.

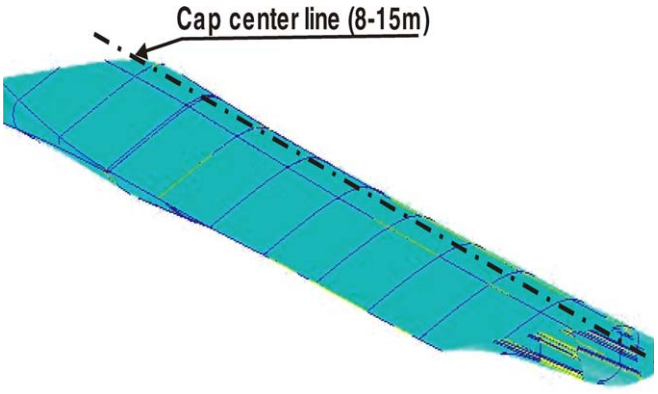

Fig. 8a. Cap centreline.

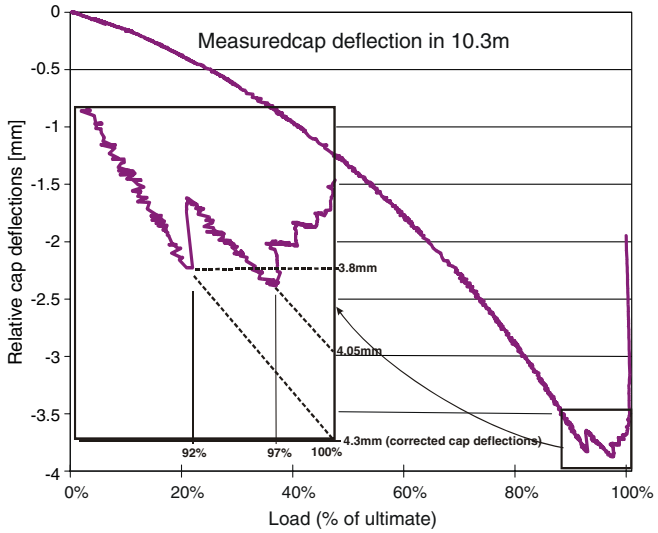

Fig. 7c. Measurements that show skin peeling and corrected cap values.

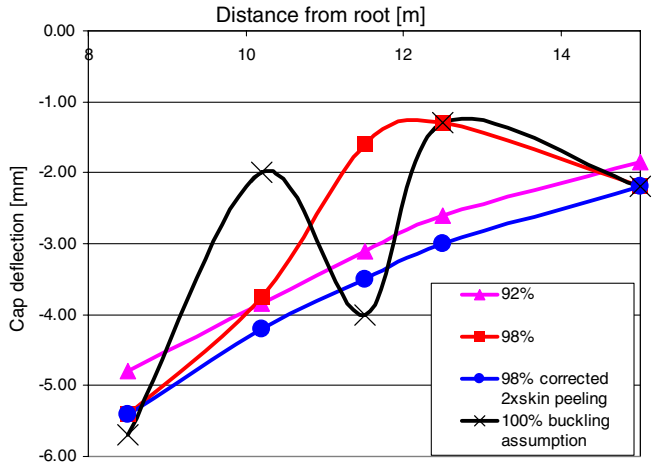

Fig. 8b. Cap deformation at different load levels.

Fig. 9. Buckling collapse.

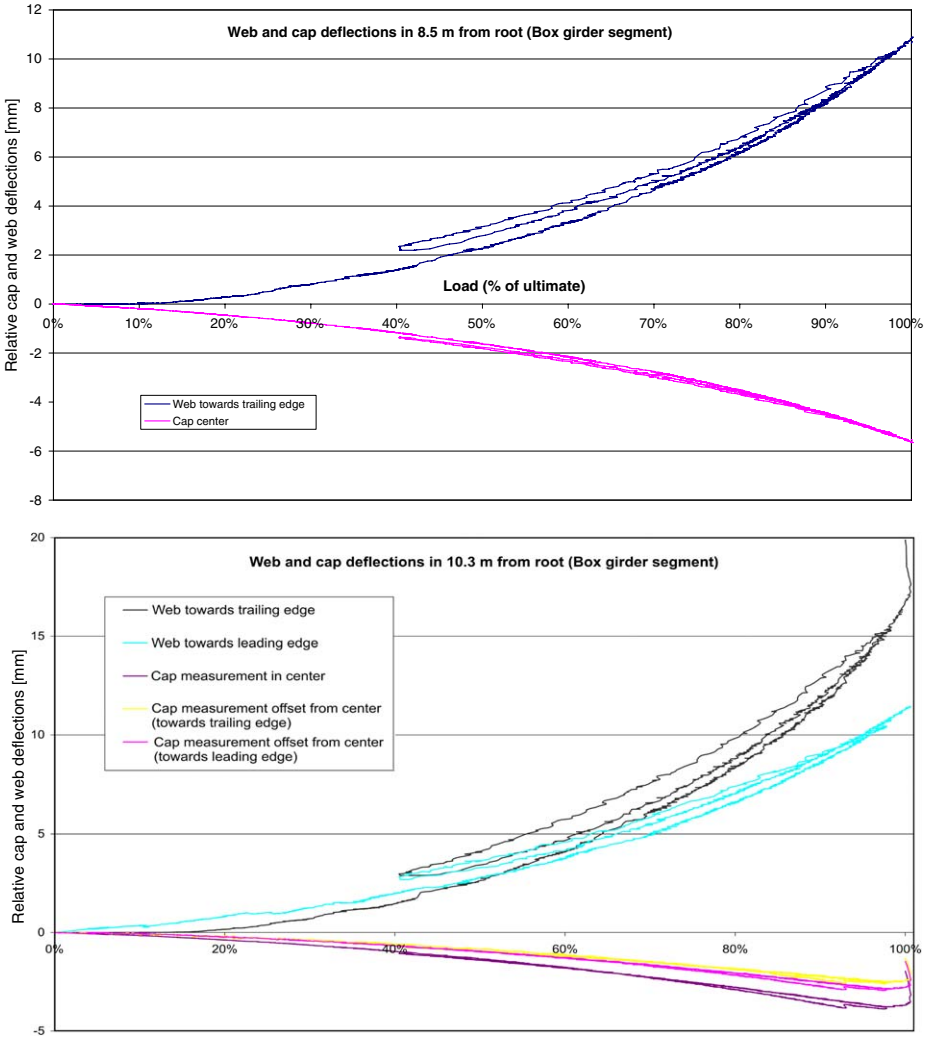

Fig. 10. Measured web and cap deflections at 8.5 m (top) and 10.3 m (bottom).

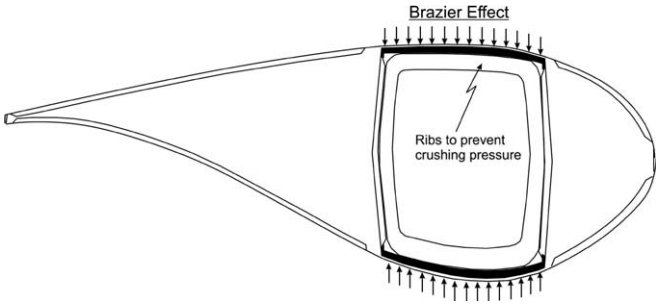

Fig. 11. Rib/bulkhead to prevent crushing pressure.

11.5 m where the final failure occurred, so cap deformation at this section is assumed. If the deformation is corrected from the skin peeling mentioned above, the cap in the longitudinal direction behaves in a smooth manner until 98% load is reached. Above this load, most likely the cap starts to buckle as shown in Fig. 8b (dark line – 100% load). This assumption is based on two observations; pictures of the blade after collapse (as in Fig. 13) and the cap measurement in 10.3 m, 12.5 m and 15.2 m which fit into this buckling pattern, see Fig. 8b.

The buckling assumption does not take the clamp at 13.2 m into account, see Fig. 9. This approximation may affect the buckling pattern since the cap is not able to buckle outwards at this location while inwards deformation is unconstrained. The inwards displacement actually looks smooth and fits into the deformation pattern up to the ultimate buckling load, see the blue (●) and pink (▲) line in Fig. 8b.[1]

The skin peeling assumption and the final buckling behaviour assumption can be confirmed by checking other measurements (strain gauges and web deflection sensors) in this segment of the wind turbine blade. Unfortunately, web sensors were only placed at 8.5 m and 10.3 m and no web measurements were taken at 12.5 m and 15.2 m.

Measurements from both sections at 8.5 m and 10.3 m support the skin peeling assumption and the buckling assumption. At 92% load where skin peeling starts, there is no sign of sudden displacement jumps in the webs at either of the sections. Displacement jumps in the cap are seen at 10.3 m but not at 8.5 m. This ties in with what one would expect from skin peeling occurring at 11.5 m, i.e. only cap deflection is affected at the nearest measuring station. The web towards the trailing edge shows a moderate increase in deflection at the 8.5 m station and a much more pronounce increase at the 10.3 m station as the load approaches ultimate. This does to some degree also confirm that buckling occurs further outboard of the 10.3 m station. Alternatively, the web may have failed locally leading to buckling in the cap. Wing structures used in the aeronautical industry (helicopter blades and fixed aircraft wings) are usually designed with the trailing edge web stronger than the web towards the leading edge. Perhaps this should also be considered in the design of wind turbine blades. Another obvious difference between wind turbines blades and aircraft wings is the lack of internal ribs/bulkheads in the wind turbine blades. This should also be considered eventhough these ribs/bulkheads may add complexity to the manufacturing process. An example of how a web/bulkhead could be incorporated in the existing blade design is shown in Fig. 10 (Fig. 11).

[1] For interpretation of colour in Figs. 1, 4, 5, 7–10, and 12–15, the reader is referred to the web version of this article.

8. Finite element results

In this section results from the numerical modelling (FEM) will be presented. The main focus will be on the 8–13 m section, where the collapse occurred.

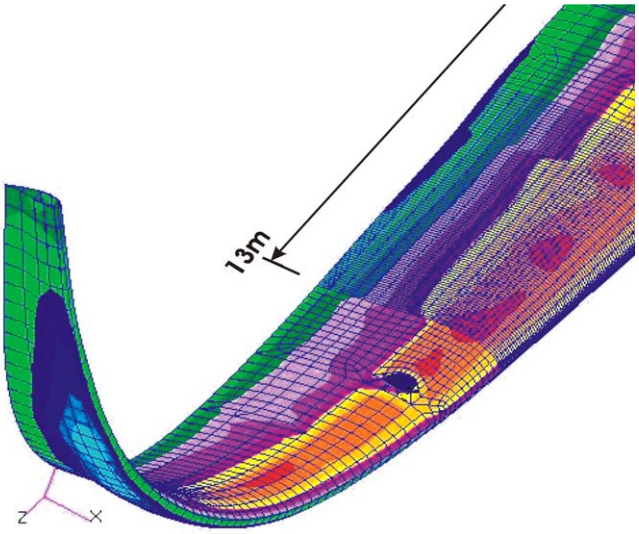

Fig. 12a. Global 34 m FE-model.

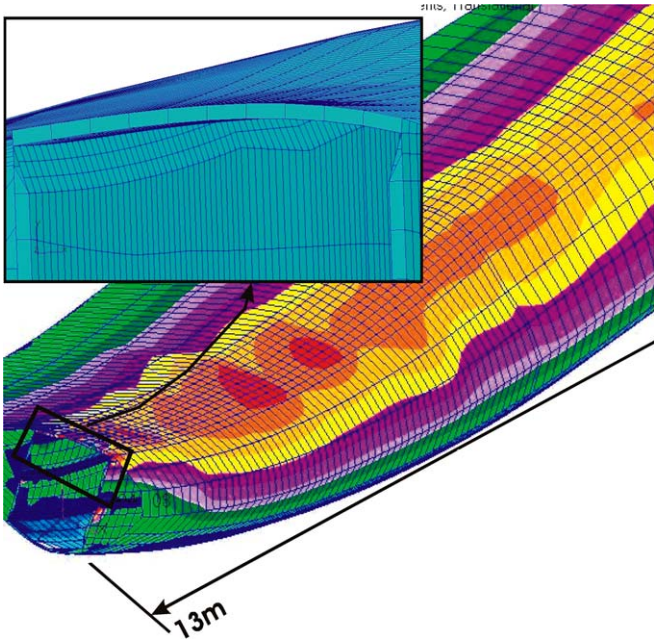

Fig. 12b. 0–13 m sub-model.

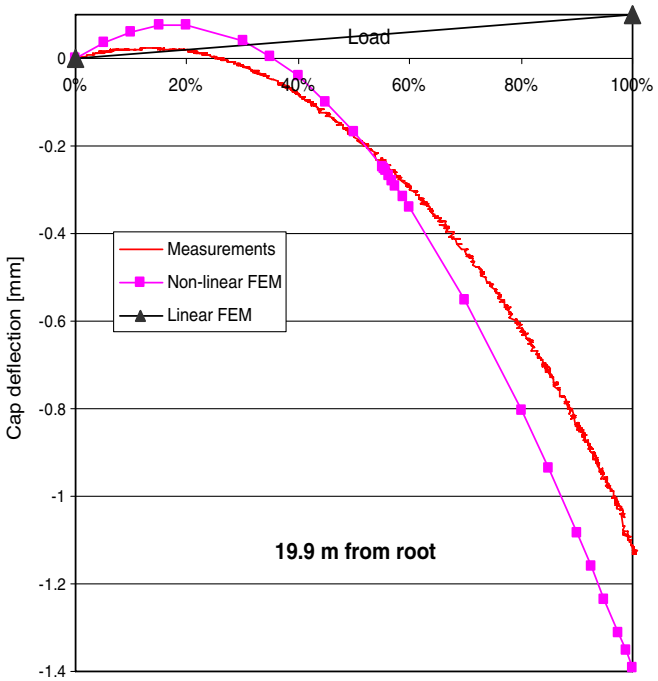

Fig. 13. Non-linear response in global model.

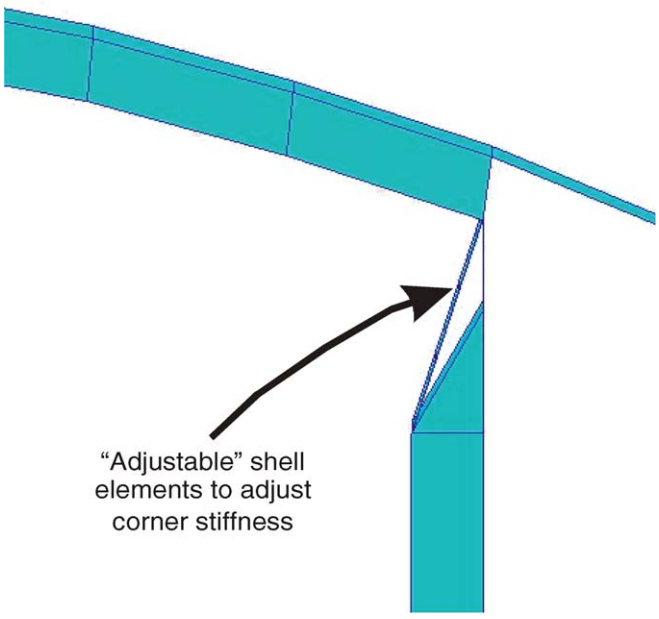

Fig. 14b. Box corner used for calibration.

8.1. 0–13 m sub-model

Capturing the correct deformation pattern required a more detailed sub-model of the 0–13 m section. The detailed sub-model includes solid elements in the webs and spar caps, see Fig. 12b.

The main purpose of a global FE-model of the whole blade is to provide representative boundaries for the 0–13 m sub-model. Non-linear analysis is clearly necessary here due to the large deflections seen in the blade at higher loads. More interestingly, a combination of the anticlastic effect [3], which is a linear phenomenon, and the non-linear Brazier effect [4,5] seem to counteract one another at certain locations along the blade. At small loads the anticlastic

Fig. 14a. Section through a box corner.

effect can cause outward cap deflection which then changes to inward deflection at higher loads as the Brazier effect (ovalization) takes over. This observation is illustrated in Figs. 12a and 12b. Linear analysis would simply not capture deflections due to the Brazier effect (Fig. 13).

9. Calibration of corner stiffness in the FE-model

Working with large wind turbine blades, made of fibre composites, a large margin of production tolerances must be accepted. SSP-Technology A/S uses a relative high quality production method (pre-preg without autoclave). Imperfections, such as voids, are most pronounced in areas where pre-preg layers terminate such as the corner of a box girder (Figs. 14a and 14b).

In principle all variations could be identified by cutting the blade into small pieces, measure the local stiffness, and then make a detailed FE-model which includes all these variations. In practise this is prohibitively expensive and a simpler approach was applied. Box girder corners in the FE-model were only represented with a coarse mesh of layered shell elements, which of course do not give the true picture of the corner stiffness. However, the modulus of an "adjustable" element was tuned to obtain the best fit with the actual deflections measured in the full-scale test.

10. Comparison of experimental test and numerical modelling

Comparing experimentally measured cap deflections with FE predictions, the agreement is found to be acceptable following calibration of the corner stiffness, see Fig. 15a. The web deflections, however, are not satisfactory above 80% load, see Fig. 15b. It was not possible to obtain better results by further adjustment of the corner stiffness and other improvements must be considered in the future work. It appears that a geometrical softening mechanism

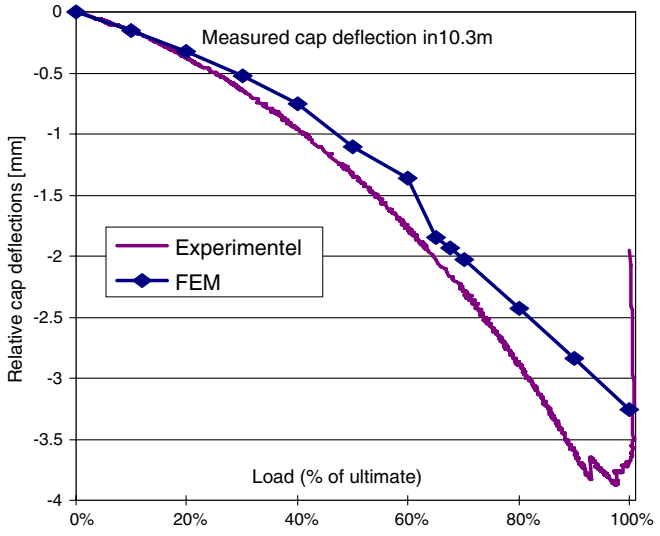

Fig. 15a. Comparison of cap deflections.

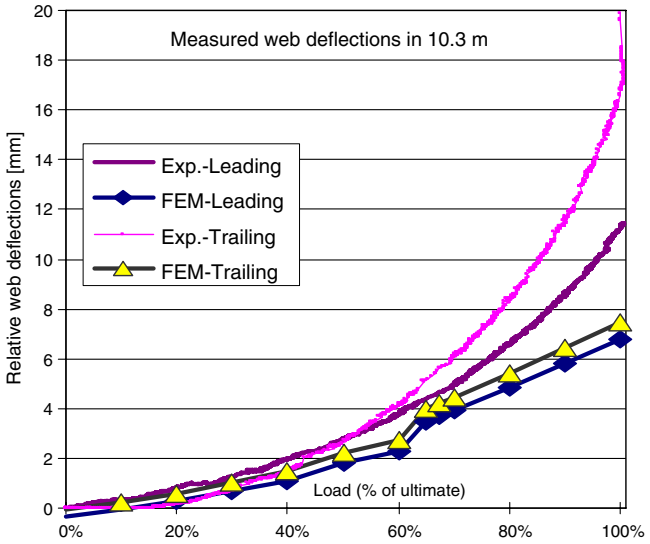

Fig. 15b. Comparison of web deflections.

or material non-linearity exists in the actual blade. This is not accounted for in the FE-model hence good correlation is seen at lower loads while the FE-model is over-stiff at higher loads approaching ultimate strength. Also, a kink is evident on the FE deflection curves at 60% load which is hardly noticeable on the curves obtained from the test. If certain features in the FE-model are too stiff it is conceivable that localized post buckling or snap-through has a more pronounced effect on the lateral deflections of the box girder. It should be mentioned that the overall flap-wise blade deflection shows exact agreement between test and FE-model. This is also the case for natural vibration modes, which are not included in this paper.

If the accuracy of the local FE-results are to be improved, manufacturing imperfections must be included in the FE-model. For the blade in question, the section at 10.3 m turned out to have a relatively large geometric imperfection in the load carrying cap which one would expect to influence local deformation behaviour.

11. Conclusion

Non-linear finite element analyses of a 34 m wind turbine blade with a load carrying box girder and loaded in flap-wise bending have revealed a variety of behaviour along the span. The Brazier effect dominates outwards of the 8 m section. This non-linear effect was also found to dominate at the 13 m section where the boundary conditions from the global FE-model were applied to a local FE-model. This ties in with the requirement for a non-linear global FE-model.

Simulation of local behaviour relied on calibration of the FE-model, mainly due to the variations in production. Especially corners in the box girder show large variations, hence the sub-model did not include fine details, but was calibrated against measured local deformations from the full-scale test.

Measurements supported by FE-results also show that debonding of the outer skin was the initial failure mechanism followed by delamination buckling which led to collapse. When the skin debond reaches a certain size the buckling strength of the load carrying laminate becomes critical and final collapse occurred.

12. Future work

The skin debonding failure, observed in the full-scale test, will be investigated further using computational methods. It is intended to use fracture mechanics based cohesive interface elements in a finite element model. These elements are capable of predicting both initiation and propagation of a delamination.

Extensive delamination was observed in the failed blade and this failure mode was due to interlaminar tensile stress caused by straightening of the curved caps. This deformation is a result of the crushing pressure from the Brazier effect. This failure mode will be studied in more detail also by the use of cohesive elements in a finite element model.

Finally, in this paper only the displacement measurements are presented but strain measurements were also recorded throughout the loading history and will be compared with the FE-results.

References

[1] Jørgensen ER, Borum KK, McGugan M, Thomsen CL, Jensen FM, Debel CP. Full scale testing of wind turbine blade to failure – flapwise loading. Risø-R-1392(EN) ISBN 87-550-3184-6; ISBN 87-550-3185-4 (Internet) ISSN 0105-2840.

[2] Jensen FM. Compression strength of a fibre composite main spar in a wind turbine blade. Risø-R-1391(EN) ISBN 87-550-3184-6; ISBN 87-550-3185-4 (Internet) ISSN 0105-2840.

[3] Swanson SR. Anticlastic effects and the transition from narrow to wide behaviour in orthotropic beams. Comp Struct 2001;53:449–55.

[4] Brazier LG. The flexure of thin cylindrical shells and other 'thin' sections, Late of the Royal Aircraft Establishment. Reports and Memoranda, No. 1081 (M.49), 1926, p. 1–30.

[5] Cecchini LS, Weaver PM. The Brazier effect in multi-bay aerofoil sections, University of Bristol, UK.